THE JOURNAL OF BIOLOGICAL CHEMISTRY VOL. 287, NO. 49, pp. 41103–41117, November 30, 2012

A Novel Regulatory Factor Recruits the Nucleosome Remodeling Complex to Wingless Integrated (Wnt) Signaling Gene Promoters in Mouse Embryonic Stem Cells*[S]

Received for publication, September 4, 2012, and in revised form, October 10, 2012 Published, JBC Papers in Press, October 16, 2012, DOI 10.1074/jbc.M112.416545

Jeffrey J. Kim[‡§1], **Omar Khalid**[‡§1], **Sheynie Vo**[‡], **Ho-hyun Sun**[‡], **David T. W. Wong**[§¶], **and Yong Kim**[‡§¶2]

From the [‡]*Laboratory of Stem Cell and Cancer Epigenetic Research, UCLA, Los Angeles, California 90095, the* [§]*Dental Research Institute, School of Dentistry, UCLA, Los Angeles, California 90095, and the* [¶]*Jonsson Comprehensive Cancer Centre, UCLA, Los Angeles, California 90095*

Background: Nucleosome remodeling is integral in transcriptional control, yet the exact mechanisms involved remain to be elucidated.
Results: CDK2AP1 is a novel regulatory factor that guides the NuRD complex.
Conclusion: CDK2AP1 guides NuRD onto promoters involved in Wnt signaling of mouse embryonic stem cells.
Significance: Understanding NuRD regulation is critical in understanding transcriptional regulation.

The nucleosome remodeling and deacetylation (NuRD) complex is required for modulating the transcription of essential pluripotency genes in ESC self-renewal. MBD3 is considered a key player in the formation of a functional NuRD complex. The recruitment of MBD3 to methylated promoters may require other prerequisite factors. We show that cyclin-dependent kinase 2-associated protein 1 (CDK2AP1), an essential gene for early embryonic development, plays a role in pluripotency of ESC by engaging MBD3 to the promoter region of Wnt signaling genes. The occupancy of MBD3 on several promoters of Wnt genes was significantly lost in the absence of CDK2AP1, resulting in hyperactivation of Wnt. We propose that the transcriptional modulation of the Wnt pathway mediated by NuRD requires the presence of essential auxiliary components such as CDK2AP1, which may aid the association of the complex with specific focal regions of the target promoters.

Embryonic stem cells (ESCs)[3] are pluripotent cells with self-renewal capabilities and the ability to differentiate into all cells in the body. ESCs have significant potential to provide regenerative therapies in wide ranges of diseases (1–5); however, one of the major hurdles in stem cell-based therapies is controlling lineage commitment to treat a particular disease (6). ESCs *in vivo* receive carefully orchestrated signals from surrounding tissues to guide the future embryo down a correct developmental pathway (7, 8). Thus, to understand how ESCs self-renew and differentiate, it is imperative to identify these guiding signals and their regulation.

Recent studies have shown that epigenetic mechanisms play a key role in the pluripotency of ESCs (9–11). Correlations between differentiation status of stem cells and epigenetic changes are well known (12–14). It has been shown that the control of DNA methylation mediates the assembly of chromatin during early embryogenesis and the formation of chromatin structure (15, 16). The nucleosome remodeling and deacetylase (NuRD) is a multisubunit transcriptional modulator that plays a role in chromatin remodeling and histone deacetylation (17). In mice, NuRD-mediated silencing has been implicated in the cell fate decisions in stem cells (18). One of the major NuRD components is methyl-binding domain protein 3 (MBD3), which recognizes methylated DNA (17). *Mbd3*-deficient ESCs, which are viable but fail to form a stable NuRD complex, are severely compromised in the ability to differentiate and show Leukemia Inhibitory Factor (LIF)-independent self-renewal (18).

Cyclin-dependent kinase 2-associated protein 1 (CDK2AP1) was first discovered as a putative tumor suppressor gene in oral cancer (19, 20). Targeted deletion of *Cdk2ap1* leads to an embryonic lethality between 3.5–5.5 days post coitum (d.p.c.) (21). Interestingly, *Cdk2ap1*$^{-/-}$ mESCs fail to differentiate, and show Leukemia Inhibitory Factor (LIF)-independent self-renewal, remarkably similar to *Mbd3*-deficient mESCs (18, 22, 23). Recently, using a proteomic approach, CDK2AP1 has been identified to be a core subunit of NuRD (24). Moreover, the interaction of CDK2AP1 with MBD3 is required for epigenetic silencing of *Oct4*, which has been shown to be essential in the self-renewal of ESCs (22). Therefore, we hypothesized that *Cdk2ap1* is required in the epigenetic regulation of ESCs, and deletion of *Cdk2ap1* leads to changes in NuRD-dependent DNA methylation and corresponding gene expression. Furthermore, we hypothesized that deletion of *Cdk2ap1* affects the structural integrity of NuRD and that is partly responsible for the loss of differentiation potential in *Cdk2ap1*$^{-/-}$ mESCs.

* This work was supported by a California Institute of Regenerative Medicine grant (Basic Biology Award II, RB2-01562) (to Y. K.) and National Institutes of Health, NIDCR Grants R01DE014857 (to D. T. W. W.), F30DE020003 (to J. J. K.), and T32DE07269 (to O. K.).
[S] This article contains supplemental Tables S1–S5 and Fig. S1.
[1] Both authors contributed equally to this work.
[2] To whom correspondence should be addressed: Laboratory of Stem Cell and Cancer Epigenetic Research, UCLA, 10833 Le Conte Ave., 73-035 CHS, Los Angeles, CA 90095. Tel.: 310-825-7210; Fax: 310-825-0921; E-mail: thadyk@ucla.edu.
[3] The abbreviations used are: ESC, embryonic stem cell; WGCNA, weighted correlation network analysis; TSS, transcriptional start site; DAVID, database for annotation, visualization, and integrated discovery; APC, adenomatous polyposis coli; NuRD, nucleosome remodeling and deacetylation; TCF-LEF, T cell factor-Lymphoid enhancer factor.

Here, we show for the first time that NuRD epigenetically regulates the expression levels of Wnt genes in mESCs. We find that the molecular interaction between MBD3 and CDK2AP1 is essential for the epigenetic regulation of the Wnt signaling pathway in mESCs. This may have significant implications because Wnt and the self-renewal ability of ESCs are closely related (25–29).

We provide comprehensive biological interactions among NuRD, Wnt signaling, and mESC differentiation in a global genomic context. The interaction map uncovers new gene coexpression patterns, which modulate stem cell pluripotency. Taken together, we propose a model that shows there are essential auxiliary components, such as CDK2AP1, that aid the association of the NuRD complex to specific promoters and mediate epigenetic regulation of regions of importance in controlling genes responsible for stem cell pluripotency.

EXPERIMENTAL PROCEDURES

Mouse Embryonic Stem Cell Line and Culture Conditions—mESCs (129/Sv6129/Sv-CP; UCLA Stem Core) F1 were cultured on a γ-irradiated mouse embryonic fibroblast (MEF) feeder cell layer with mESC medium (consisting of 410 ml of DMEM high-glucose (HyClone, Logan, UT), 70 ml of knockout serum replacement (Invitrogen), 5 ml of 100× NEAA (Invitrogen), 5 ml of 100× penicillin/streptromycin (Invitrogen), 5 ml of 100× glutamine (Invitrogen), 5 ml of 100× HEPES buffer (Invitrogen), 50 μl of β-mercaptoethanol (0.1 mM), and 200 μl of Leukemia Inhibitory Factor (LIF) (1000 units/ml)). mESC cultures were incubated at 37 °C, 5% CO_2. Before mESCs were collected for subsequent experiments, they were passaged a minimum of two times without additional mouse embryonic fibroblast feeder cells and went through differential attachment on low attachment plates (Kord-Valmark, Brampton, Ontario).

Methyl-DNA Immunoprecipitation and DNA Methylation Array Analysis—Genomic DNA was isolated according to a standard protocol (30). Genomic DNA was sheared by sonication (20% ampere, 5 pulses with 10 s of sonication and a 1-min pause) to generate fragments between 300 bp to 1000 bp. Sonication efficiency was confirmed by electrophoresis.

Methyl-DNA immunoprecipitation was performed as described previously (31). Briefly, 4 μg of sonicated DNA was resuspended in 430 μl of Tris-EDTA, pH 8.0. DNA was denatured for 10 min at 100 °C. DNA was immunoprecipitated using antibody against 5-methylcytidine (Eurogentec, San Diego, CA). After a 2-h incubation, 40 μl of prewashed Dynabeads with M-280 sheep anti-mouse IgG antibody (Invitrogen) was added to the denatured DNA. Dynabeads and DNA were incubated for 2 h in 4 °C and subsequently washed with 700 μl of 1× IP buffer for 10 min at room temperature. Beads were resuspended in 250 μl of proteinase K digestion buffer and incubated for 3 h at 50 °C. Methylated DNA was purified by phenol/chloroform extraction followed by ethanol precipitation. The pellet was dissolved in 60 μl of Tris-EDTA, pH 8.0 buffer.

Genomic profiling was performed by NimbleGen Systems (Mouse Methylation 3X720K CpG RfSq Promoter Array-MM9). Arrays covered 2950 bp upstream and 740 bp downstream tiling for each promoter of 20,404 mouse genes. Average probe length was 50–75-mer, and median probe spacing was 100 bp. 3 mg of sonicated DNA as input and 4 mg of 5-methylcytidine antibody pulldown DNA samples were sent to NimbleGen Systems for differential labeling by priming with Cy3 or Cy5 and hybridization to arrays.

From the scaled $\log_2$ ratio data, a fixed-length window (750 bp) was placed around each consecutive probe, and the one-sided Kolmogorov-Smirnov (KS) test was applied to determine whether the probes were drawn from a significantly more positive distribution of intensity log ratios than those in the rest of the array. Resulting score for each probe was $-\log_{10} p$ value from the windowed KS test around that probe and was assigned as "p value." NimbleScan software (NimbleGen Systems) detects peaks by searching for at least two probes above a p value minimum cutoff ($-\log_{10}$) of 2. Peaks within 500 bp of each other are merged and annotated to the nearest gene. Data were visualized using SignalMap software (NimbleGen, Madison, WI), analyzed further by Galaxy (Penn State, University Park, PA) and annotated by DAVID functional annotation bioinformatics microarray tools (32).

Western Blotting and Immunofluorescence—After purification of protein samples according to the standard protocol, the concentration of protein quantification was determined using NanoDrop 1000 Spectrophotometer (Thermo Scientific, Waltham, MA). SDS-PAGE gel electrophoresis and blotting was performed as described (33). Membranes were blocked in 3% milk in Tris-Buffer Saline with 0.1% Tween 20 and probed with the following antibodies: anti-CDK2AP1 monoclonal antibody (1:3000, Epitomics, Burlingame, CA, 2910-1), anti-p-β-catenin antibody (1:1000, Developmental Studies Hybridoma Bank, Iowa City, IA, PY489), anti-total β-catenin polyclonal antibody (1:1000, Abcam, Boston, MA, ab6302), anti-GSK3β polyclonal antibody (1:3000, Applied Biological Materials, Richmond, Canada, Y021002), anti-p-GSK3β-Tyr-216 (1:3000, Applied Biological Materials, Richmond, Canada, Y011301), anti-AXIN1 (1:3000, Cell Signaling, Danvers, MA, 2075), and anti-tubulin polyclonal antibody (1:10,000, Abcam, Boston, MA, ab6160) for overnight at 4 °C. Membranes were then washed with Tris-Buffer Saline with 0.1% Tween 20 followed by incubation with horseradish peroxidase-conjugated secondary antibody (GE Healthcare, NA931V and NA934V) for 1 h at room temperature. Membranes were developed with an enhanced chemiluminescence (ECL) chemiluminescence reagent (Amersham Biosciences) and HyBlot CL films (Denville Scientific, South Plainfield, NJ).

For immunofluorescence, cells were fixed in 100% methanol for 15 min at room temperature. For staining, samples were permeabilized for 15 min in freshly prepared PBS containing 0.25% Triton X-100 and then blocked for 1 h in 5% donkey serum, 0.1% fish gelatin, 0.2% Tween 20, and PBS. Samples were then incubated in 37 °C water bath for 1 h with 1 mg/ml of primary antibody diluted in blocking solution. Samples were transferred to a 1:500 dilution of goat anti-mouse IgG rhodamine (Thermo Scientific) and goat anti-rabbit IgG fluorescein in blocking solution and incubated in a 37 °C water bath for 1 h. Stem cells were mounted on a glass slide with mounting medium with DAPI (Vectashield, Burlingame, CA) and visualized with an inverted light microscope (Olympus IX81 and CellSens Dimension software, Center Valley, PA).

Transfection and Luciferase Reporter Assay—Cells were seeded in 48-well plates at 1×10^5 cells/well. The following day cells were transiently transfected with 600 ng of TCF-LEF reporter construct and 600 ng of pCMV-*Renilla* luciferase per well, using Lipofectamine 2000 reagent according to the manufacturer's instructions for 12 h (Invitrogen). Transfection of 600 ng of empty vector was paralleled as negative control. LiCl (10 mM) was used to activate TCF-LEF. Transfected cells were lysed with 1× passive lysis buffer in Dual-Luciferase reporter assay kit (Promega, San Luis Obispo, CA). 100 μl of LAR II was added into each lysate. Firefly luciferase activity was measured by BioTek Synergy HT Microplate Reader (BioTek, Winooski, VT). 100 μl of Stop & Glo reagent was dispended into each well. Renilla was measured by the BioTek plate reader.

Quantitative RT-PCR—Total RNA was purified from undifferentiated WT mESCs and undifferentiated CDK2AP1$^{-/-}$ mESCs, using the RNeasy kit (Qiagen, Valencia, CA) to eliminate contaminating genomic DNA; this was followed by DNase treatment (Promega, San Luis Obispo, CA) of eluted RNA. cDNA was synthesized using iScript cDNA Synthesis kit (Bio Rad, Hercules, CA) according to the manufacturer's protocol. For the PCR reactions, 2× LightCycler 480 SYBR Green I Master Mix (Roche Applied Science) was used with the LightCycler 480 RT-PCR machine (Roche Applied Science). Reactions were done in triplicate using 1 μl of cDNA as a template in a 20-μl reaction volume. The amount of starting cDNA was normalized to GAPDH. Each reaction was repeated three times.

Gene Expression Array—RNA was isolated and prepared according to the standard protocol by the Clinical Microarray Core at UCLA. Affymetrix GeneChip Mouse Genome 430 2.0 Array (Affymetrix, Santa Clara, CA) was used for the gene expression studies. Microarray data analysis was performed using R software. Raw expression data were $\log_2$ transformed and normalized. Data quality control was verified by high inter-array correlation (Pearson correlation coefficients > 0.85) and detection of outlier arrays based on mean inter-array correlation and hierarchical clustering. Probes were considered robustly expressed if the detection p value was <0.05 in duplicate samples.

WGCNA and Network Construction—Weighted correlation network analysis (WGCNA) was performed by following the tutorial written by Langfelder and Horvath (34). Unsigned co-expression networks were built using the WGCNA package in R software. Clusters of genes that behaved similarly, termed module eigengenes, were grouped together into different color modules. The modules were related to traits (WT *versus* KO). The significant modules were further analyzed by DAVID functional annotation.

RESULTS

Deletion of Cdk2ap1 Leads to Global Methylomic and Transcriptomic Changes—To date, the role of NuRD in transcriptional regulation, signaling, and chromatin remodeling in the context of self-renewal is not fully understood (35). We have attempted to answer the question of how NuRD is being recruited to genes and changes the fate of stem cells by using our *Cdk2ap1* ESC model system. We used this approach because we know that CDK2AP1 is a core subunit of NuRD, and deletion of *Cdk2ap1* alters the differentiation potential similar to abrogation of the NuRD complex.

We have examined both global DNA methylation and gene expression profiles affected by deletion of *Cdk2ap1* in mESCs (Fig. 1). Utilizing DNA methylation arrays, the DNA methylation profile of 20,404 known promoters and CpG islands were compared. The array revealed that there were 7,864 and 7,725 genes significantly methylated in WT and *Cdk2ap1*$^{-/-}$ mESCs, respectively (Fig. 1*a*). There were 1,525 and 1,386 genes differentially methylated in WT and *Cdk2ap1*$^{-/-}$ mESCs, respectively (Fig. 1*a*).

To examine the genome-wide changes in methylation pattern due to deletion of *Cdk2ap1*, differentially methylated genes were clustered and visualized by heat maps (Fig. 1*b*). Genes that were hypomethylated in *Cdk2ap1*$^{-/-}$ are represented in two heat maps on the *left* (Fig. 1*b*). These changes were site-specific and only occurred between −2500 bp to the transcriptional start site (TSS). Genes that were hypermethylated in *Cdk2ap1*$^{-/-}$ is represented in two heat maps on the *right*, and changes were localized between TSS and 2500 bp (Fig. 1*b*). Overall methylation intensity changed due to deletion of *Cdk2ap1*. DNA methylation intensities of differentially methylated genes were averaged and plotted against genomic location (Fig. 1*c*). It was found that methylation changes were site-specific. *Cdk2ap1*$^{-/-}$ mESCs showed hypomethylation in the promoter regions compared with WT. However, *Cdk2ap1*$^{-/-}$ mESCs showed hypermethylation in the transcribed region compared with WT (Fig. 1*c*). It is known that transcriptional silencing is mainly associated with promoter methylation; however, a major role for intragenic methylation has also been shown (36).

To delineate the functional significance of differential methylation upon deletion of *Cdk2ap1*, we performed DAVID (database for annotation, visualization, and integrated discovery) analysis (32). From the analysis, we observed six pathways with Wnt signaling as the most significant (Fig. 1*d*).

There are at least two ways in which DNA methylation can suppress gene transcription. Methylation of DNA on a promoter physically interferes with transcriptional activators from binding to the promoter. It is also known that a repressive complex such as NuRD binds to the methylated DNA and prevents transcription (37). To correlate DNA methylation and gene expression, complementary gene expression microarray analysis was performed. To identify differentially expressed genes due to deletion of *Cdk2ap1*, we performed WGCNA (Fig. 1*e*) (34). Using the WGCNA, we found clusters of genes that behaved similarly. Deletion of *Cdk2ap1* yielded 14 coexpression modules (Fig. 1*e*; *first row*). These modules were quantitatively related to two traits, WT and *Cdk2ap1*$^{-/-}$ (Fig. 1*e*; *second* and *third rows*, respectively). For example, genes in the blue module were up-regulated in WT and down-regulated in *Cdk2ap1*$^{-/-}$ (Fig. 1*e*).

We found the blue and the turquoise modules to be significantly related to the deletion of *Cdk2ap1* (Fig. 1*f*). The negative correlations of the blue module indicate down-regulation of its members with deletion of *Cdk2ap1* (Fig. 1*g*; *top*, and supplemental Table S1). In contrast, the positive correlations observed for the turquoise module indicate significant up-reg-

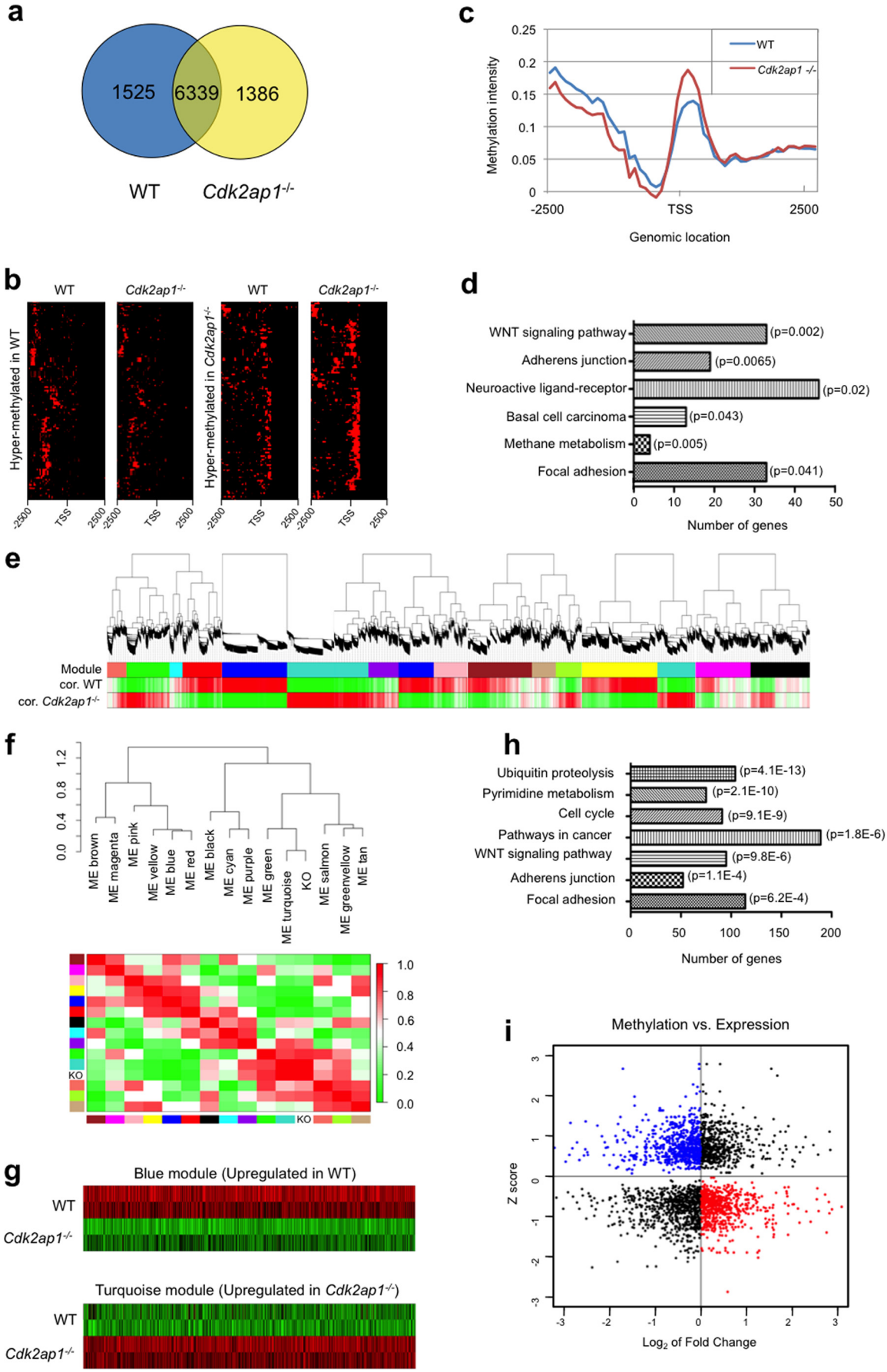
a
1525
6339
1386
WT
Cdk2ap1-/-
c
Methylation intensity
0.25
0.2
0.15
0.1
0.05
0
WT
Cdk2ap1 -/-
-2500
TSS
2500
Genomic location
b
WT
Cdk2ap1-/-
WT
Cdk2ap1-/-
Hyper-methylated in WT
Hyper-methylated in Cdk2ap1-/-
-2500
TSS
2500
d
WNT signaling pathway
(p=0.002)
Adherens junction
(p=0.0065)
Neuroactive ligand-receptor
(p=0.02)
Basal cell carcinoma
(p=0.043)
Methane metabolism
(p=0.005)
Focal adhesion
(p=0.041)
0
10
20
30
40
50
Number of genes
e
Module
cor. WT
cor. Cdk2ap1-/-
f
0.0
0.4
0.8
1.2
ME brown
ME magenta
ME pink
ME yellow
ME blue
ME red
ME black
ME cyan
ME purple
ME green
ME turquoise
KO
ME salmon
ME greenyellow
ME tan
KO
1.0
0.8
0.6
0.4
0.2
0.0
h
Ubiquitin proteolysis
(p=4.1E-13)
Pyrimidine metabolism
(p=2.1E-10)
Cell cycle
(p=9.1E-9)
Pathways in cancer
(p=1.8E-6)
WNT signaling pathway
(p=9.8E-6)
Adherens junction
(p=1.1E-4)
Focal adhesion
(p=6.2E-4)
0
50
100
150
200
Number of genes
i
Methylation vs. Expression
Z score
3
2
1
0
-1
-2
-3
-3
-2
-1
0
1
2
3
Log2 of Fold Change
g
Blue module (Upregulated in WT)
WT
Cdk2ap1-/-
Turquoise module (Upregulated in Cdk2ap1-/-)
WT
Cdk2ap1-/-

ulation with deletion of *Cdk2ap1* (Fig. 1*g*; *bottom*, and supplemental Table S2). Next, we performed DAVID analysis on these modules and found seven biological processes (Fig. 1*h*).

We examined the correlation between DNA methylation and gene expression by comparing the Z scores to the fold changes (Fig. 1*i*). Genes that were hypermethylated in the *Cdk2ap1*$^{-/-}$ mESCs with corresponding decreases in gene expression were plotted in *blue* (Fig. 1*i*; *upper left corner*). Genes that exhibited hypomethylation and corresponding increases in gene expression due to deletion of *Cdk2ap1* were plotted in *red* (Fig. 1*i*; *lower right corner*). Overall, we found that there was a 51% correlation between DNA methylation and gene expression (Fig. 1*i* and supplemental Table S3).

We performed gene ontology analysis of the two most significant modules from the expression array (Fig. 2*a*) and found that the turquoise and blue modules had similar ontological clusters. We found the most representative genes (intramodular hubs) in the modules (Fig. 2, *b* and *c*). Many of intramodular hubs were associated with the Wnt signaling pathway.

When we clustered the top 35 differentially methylated genes in the Wnt pathway, we found at least two areas where deletion of *Cdk2ap1* led to hypomethylation between −2500 bp and TSS and another area where the deletion of *Cdk2ap1* led to hypermethylation between TSS and 2500 bp (Fig. 2*d* and supplemental Table S4).

Collectively, we found that there were global methylomic and transcriptomic changes due to deletion of *Cdk2ap1* in mESCs. Deletion of *Cdk2ap1* led to site-specific methylation changes at promoters of Wnt genes. These changes may have a functional consequence on Wnt signaling molecules associated with pluripotency of ESCs.

Knockdown of Mbd3 Leads to Changes in RNA Polymerase II Binding Capacity and Alters the Wnt Signaling Pathway—CDK2AP1 has been shown to associate with nucleosome remodeling components (24, 38). We postulate that disrupting the association of CDK2AP1 with the NuRD complex, specifically MBD3, should account for the transcriptomic changes resulted from the deletion of *Cdk2ap1*. To prove this hypothesis, we have performed bioinformatics analysis by using publically available ChIP-seq data (39). We compared transcriptomic changes due to the deletion of *Cdk2ap1* with the changes due to the alteration of nucleosome remodeling components, including *Mbd3*. From our bioinformatic analysis we observed specific clusters of genes affected upon knockdown of various nucleosome remodeling components, such as *p400*, *Tip60*, *Suz12*, *Mbd3*, *Brg1*, and *Ash2* (Fig. 3*a*). Subsequently, we examined the potential significance of MBD3 on Wnt gene transcription by examining the RNA polymerase II binding on our CDK2AP1-regulated Wnt genes in *Mbd3* knockdown mESCs (Fig. 3, *b* and *c*) (39). We observed that the Wnt signaling genes transcriptionally affected by CDK2AP1 were also affected in RNA polymerase II occupancy by *Mbd3* knockdown. Interestingly, the affects occurred in distinct transcriptional regions of the proximal promoter and the first exon of the gene (Fig. 3*c*). This further suggests that MBD3 affects Wnt pathway genes not only in our model system but in others as well on specific DNA elements similar to the DNA methylation array profile in our *Cdk2ap1* mESC model.

Furthermore, we performed gene ontology analysis on the gene clusters formed by alterations in nucleosome remodeling components shown in Fig. 3*a*. Wnt signaling pathway was found as one of pathways significantly affected (Fig. 3*d*). We found several genes that were commonly affected by alteration in *Cdk2ap1* and *Mbd3* (Fig. 3*e* and supplemental Table S5). Taking all these data together, it suggests that CDK2AP1 interacts with the components of nucleosome remodeling complex and plays a role in the regulation of Wnt signaling genes.

Deletion of Cdk2ap1 Leads to Activation of Wnt Signaling Pathway—From our bioinformatic analyses, we found that genes in the Wnt pathway are epigenetically and transcriptionally affected after deletion of *Cdk2ap1*. To assess whether there was any functional consequence to these changes, we measured nuclear translocation of phospho-β-catenin (Y489), a key player in Wnt signaling activity (40). We found that the level of nuclear Y489 significantly increased in *Cdk2ap1*$^{-/-}$ mESCs compared with WT, suggesting increased Wnt signaling activity in the knock-out. However, the total pool of β-catenin was similar in both WT and *Cdk2ap1*$^{-/-}$ mESCs (Fig. 4*a*). Upon reintroduction of *Cdk2ap1* into *Cdk2ap1*$^{-/-}$ mESCs, we observed a decrease in Y489 to the level in WT mESCs, which demonstrated that the increased level of Y489 was *Cdk2ap1*-specific (Fig. 4*b*). Western blotting images were quantified and statistically analyzed.

An increase in Y489 suggested that there was more available active nuclear pool of β-catenin, however, it was not a direct indication of active Wnt signaling. Therefore, we measured the

FIGURE 1. **Deletion of *Cdk2ap1* leads to global methylomic and transcriptomic changes in mESCs.** *a*, a Venn diagram shows number of genes that are significantly methylated in WT *versus* *Cdk2ap1*$^{-/-}$. There are 7,864 methylated genes in WT (1,525 unique to WT). There are 7,725 methylated genes in *Cdk2ap1*$^{-/-}$ (1,386 unique to *Cdk2ap1*$^{-/-}$). 6,639 genes are methylated in both WT and *Cdk2ap1*$^{-/-}$. *b*, clustering analysis (single linkage uncentered correlation) of WT and *Cdk2ap1*$^{-/-}$ DNA methylation array. Deletion of *Cdk2ap1* leads to hypomethylation in one set of genes (*upper panels*) and hypermethylation in other set of genes (*lower panels*). *c*, CpG islands are usually located in promoter region (−2500 bp to TSS) and first exon (TSS to 100). Shown is methylation intensity for all differentially methylated genes of WT and *Cdk2ap1*$^{-/-}$ according to respective genomic location. *d*, DAVID analysis of differentially methylated genes shows six statically significant pathways, diseases, and biological processes, with WNT signaling pathway being most significant. *e*, relationships between network modules and *Cdk2ap1* traits. *Upper panel*, dendrogramme of 14 modules. *Leaves* along *branches* represent probes. *Lower leaves* indicate greater similarity of probe expression profiles within that module. *Lower panel* (module blocks), different color blocks represent 14 modules. *Lower panel* (two correlation bands), WT and *Cdk2ap1*$^{-/-}$ bands show correlations (*cor.*) to the corresponding modules. Positive (*red*) and negative (*green*). *f*, colors on *x* axis and *y* axis represent 14 modules in the network. For each module, the heat map shows module eigengene (*ME*) correlations to traits. *Scale bar* (*lower right*) shows the range of possible correlations from positive (*red*) to negative (*green*) between two modules. *g*, heat map of module eigengenes of two modules that were significantly related to deletion of *Cdk2ap1* after Bonferroni correction (the *blue* and the *turquoise* modules). The negative correlations observed for the *blue* module (6,908 known genes) indicate significant down-regulation with deletion of *Cdk2ap1*. In contrast, the positive correlations of the turquoise (7,883 known genes) indicate up-regulation of its members with deletion of *Cdk2ap1*. *h*, DAVID analysis of modules that are most significantly related to *Cdk2ap1* reveals seven statically significant pathways, diseases, and biological processes. *i*, DNA methylation and gene expression comparison. *x* axis represents $\log_2$ of fold change (*Cdk2ap1*$^{-/-}$/WT). *y* axis represents Z score (positive, hypermethylation; negative score, hypomethylation). The *blue* and *red* plotted genes have matching DNA methylation pattern and gene expression (51%).

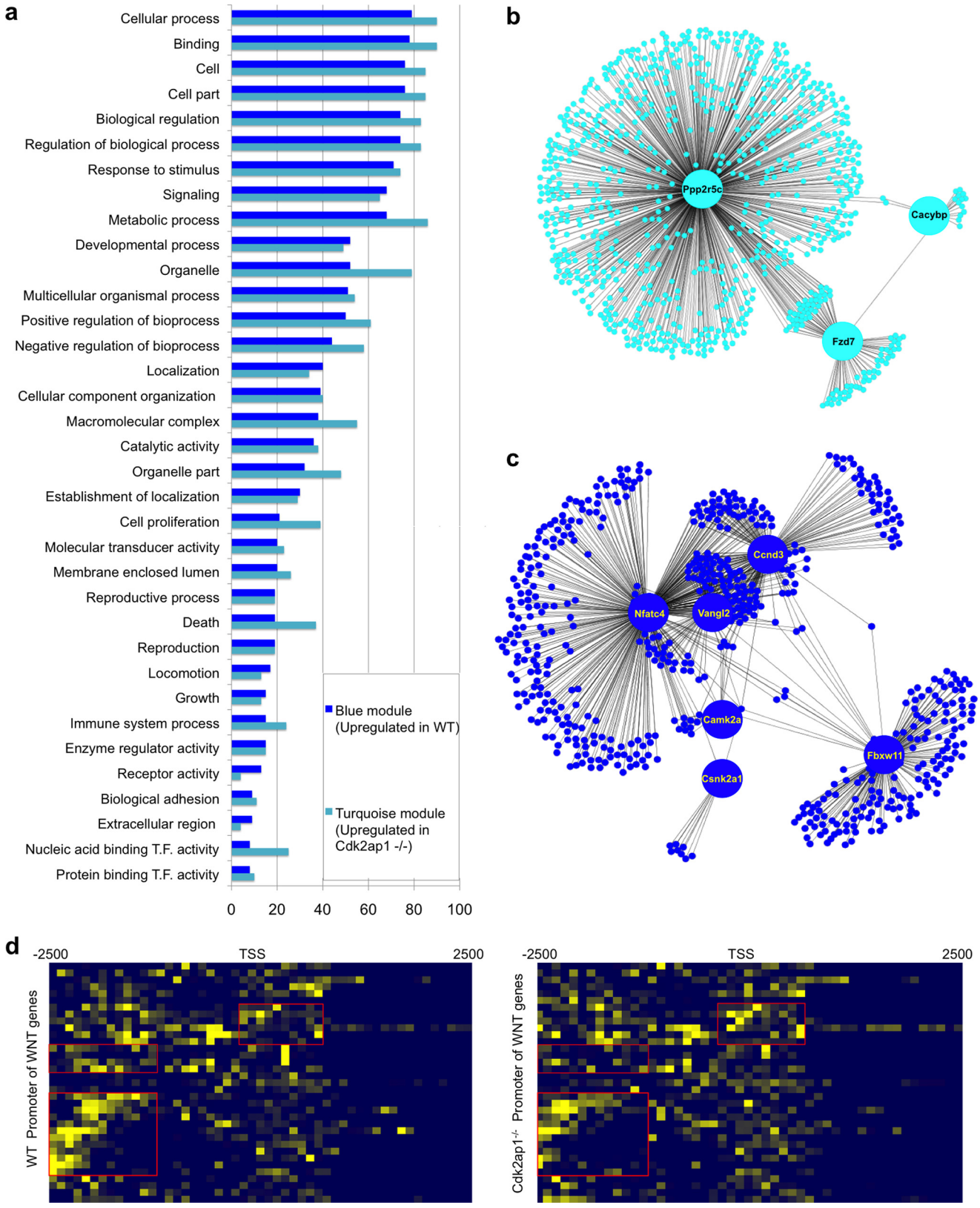

FIGURE 2. **Deletion of *Cdk2ap1* leads to alteration of DNA methylation and gene expression in Wnt signaling pathway.** *a*, relevant gene ontology categories enriched in the *blue* module and *turquoise* module. *T.F.*, transcription factor. *b*, the top 1000 connections are shown for the *turquoise* module. *Ppp2r5c*, *Cacybp*, and *Fzd7* have the highest correlation with the module eigengene value (intramodular hubs) are shown in larger size with names. *c*, the top 1000 connections are shown for the *blue* module. *Nfat5*, *Vangl2*, *Ccnd3*, *Camk2a*, *Csnk2a1*, and *Fbxw11* have the highest correlation with the module eigengene value (intramodular hubs) are shown in larger size with names. *d*, clustering analysis (single linkage uncentered correlation) of DNA methylation patterns of 35 Wnt gene promoters (WT *versus* *Cdk2ap1*$^{-/-}$) *x* axis represents genomic location from −2500 bp to 2500 bp. Most differentially methylated regions are highlighted in *red boxes*. *y* axis is listed in supplemental Table S4.

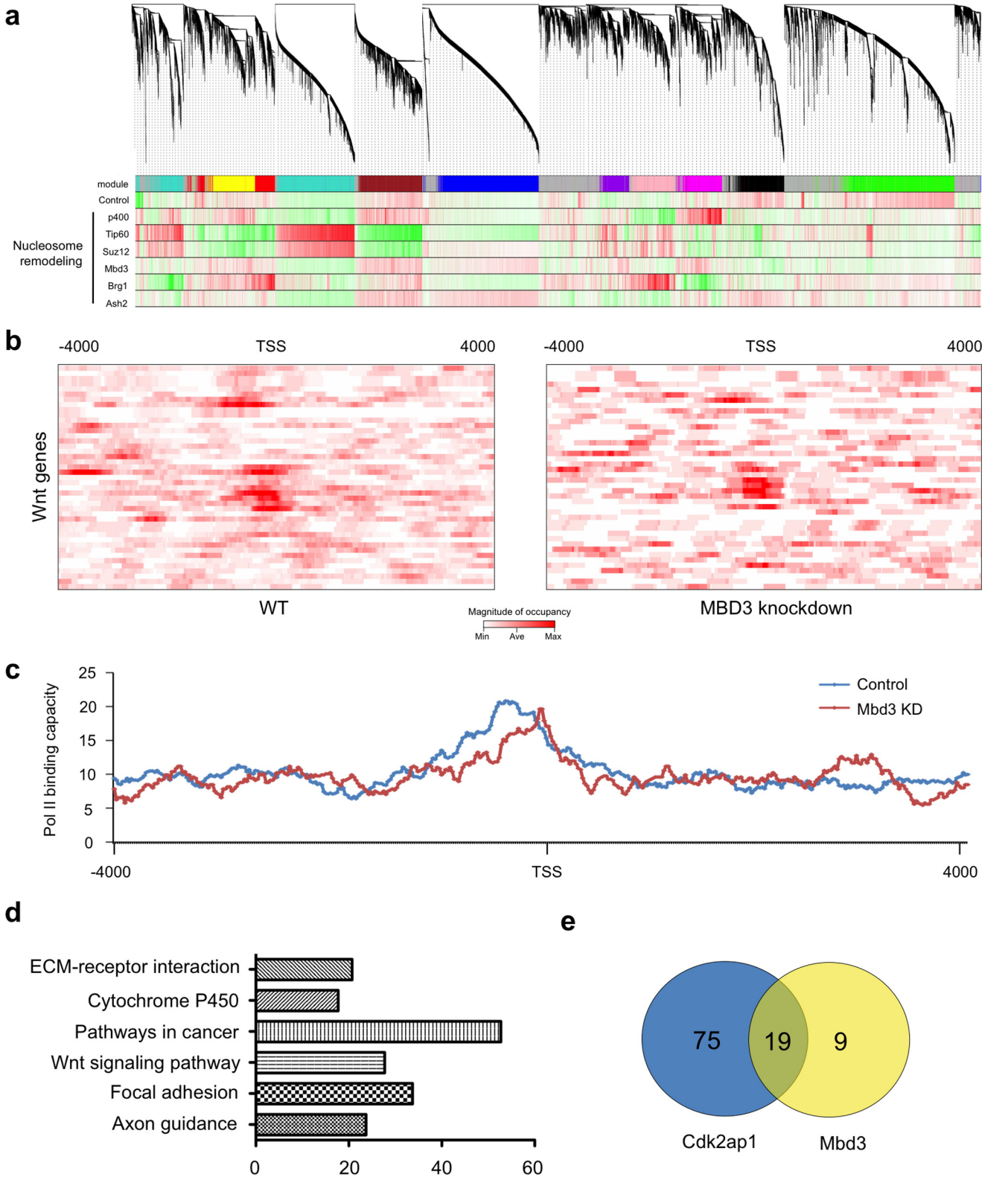

FIGURE 3. **Bioinformatic analysis of transcriptomic changes upon alteration of nucleosome remodeling complex compared with *Cdk2ap1*$^{-/-}$.** *a*, WGCNA cluster analysis of transcriptomic changes upon deletion of nucleosome remodeling complexes in mESCs. *b*, heat maps representing changes in RNA polymerase II (*Pol II*) occupancy of Wnt genes due to knockdown of *Mbd3* in mESCs. CDK2AP1 also affected these Wnt genes (shown in Fig. 2*d*). Represented on the heat map is from −4000 bp to 4000 bp of each gene. *c*, average RNA polymerase II occupancy presented in *b*. *d*, DAVID analysis of the pathways implicated in the cluster of genes altered by *Mbd3* knockdown. *ECM*, extracellular matrix. *e*, Venn diagram of Wnt genes affected by deletion of *Cdk2ap1* and/or knockdown of *Mbd3*. *Min*, minimum; *Max*, maximum; *Ave*, average.

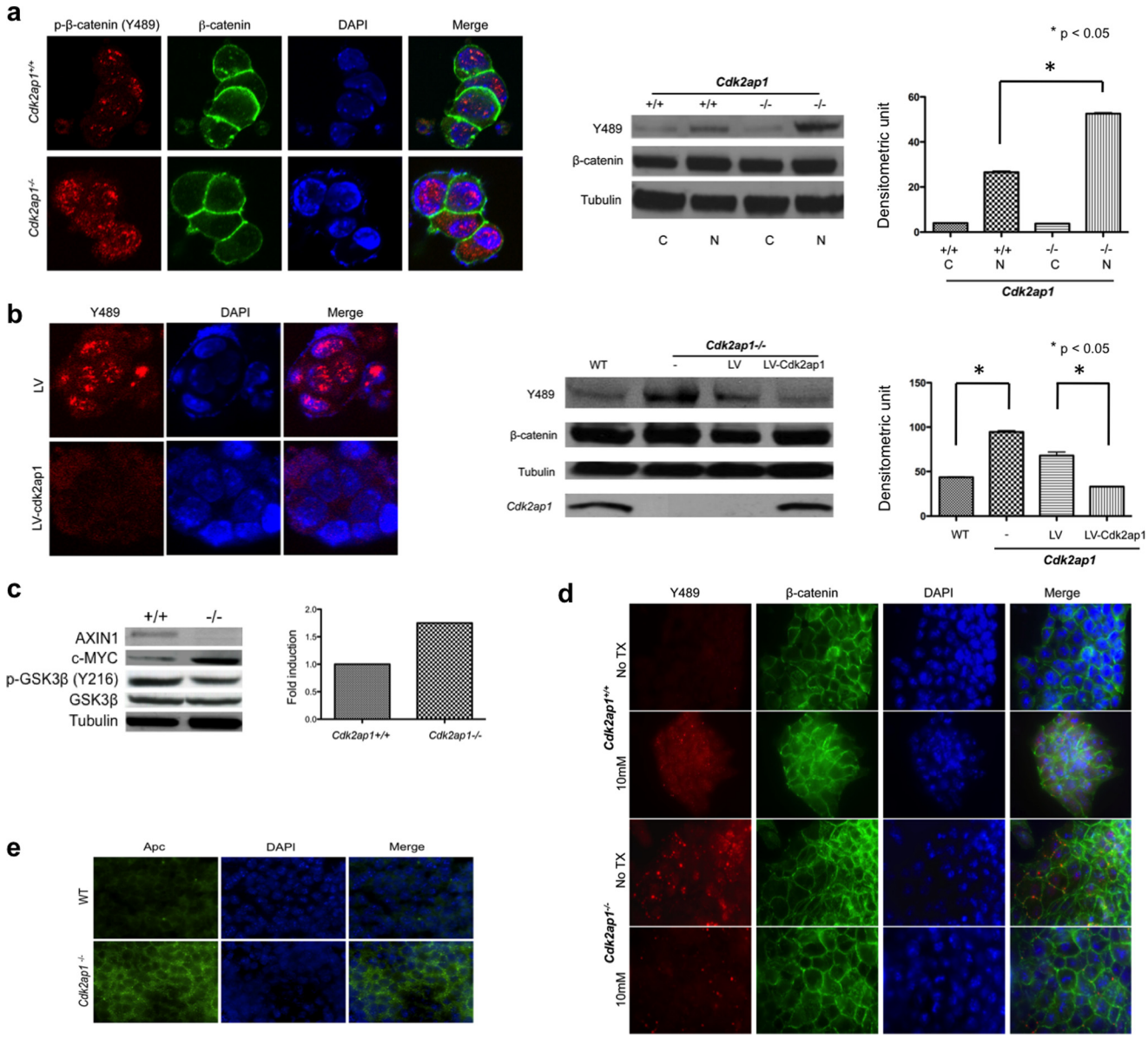

FIGURE 4. **Deletion of *Cdk2ap1* leads to deregulation of Wnt signaling pathway.** *a*, immunofluorescence microscopy for p-β-catenin (Y489) (*red*) and total β-catenin (*green*) in *Cdk2ap1*$^{+/+}$ and *Cdk2ap1*$^{-/-}$ mESCs. Western blotting analysis for Y489 (p-β-catenin) and total β-catenin. *C*, cytoplasmic fraction; *n*, nuclear fraction. Western blotting images were quantified and statistically analyzed. *b*, immunofluorescence microscopy for Y489 (*red*) in lentivirus transduction control (*LV*) and lentivirus-*Cdk2ap1* transduced *Cdk2ap1*$^{-/-}$ mESCs. Western blotting analysis for Y489, total β-catenin, and Cdk2ap1 in WT, negative control (−), lentivirus transduction control (*LV*), and lentivirus-*Cdk2ap1* transduced *Cdk2ap1*$^{-/-}$ mESCs. Western blotting images were quantified and statistically analyzed. *c*, Western blotting analysis for AXIN1, c-Myc, p-GSK3β (Y216), and GSK3β. TCF/LEF luciferase reporter assay to measure the activity of the Wnt pathway. pCMV-*Renilla* is simultaneously transfected as a control. TCF/LEF assay shows 1.75-fold induction in *Cdk2ap1*$^{-/-}$ mESCs compared with WT. *d*, Wnt signaling is activated by 10 mM LiCl. Immunofluorescence microscopy for Y489 (*red*) and total β-catenin (*green*). *Upper two rows*, WT. *Lower two rows*, *Cdk2ap1*$^{-/-}$. *e*, immunofluorescence microscopy for APC in *Cdk2ap1*$^{+/+}$ and *Cdk2ap1*$^{-/-}$ mESCs.

protein expression of upstream molecules AXIN1 and phospho-GSK3β and downstream effectors of Wnt signaling, c-Myc, and TCF-LEF activity. We found that deletion of *Cdk2ap1* led to an increase in c-Myc; a decrease in AXIN1 and phospho-GSK3β; and a 1.75-fold induction of TCF-LEF activity compared with WT (Fig. 4*c*). To determine the maximal Wnt signaling capacity in *Cdk2ap1*$^{-/-}$ mESCs, we treated WT and *Cdk2ap1*$^{-/-}$ mESCs with 10 mM LiCl. Using Y489 as a read-out, we found that Wnt signaling was activated in the WT mESCs to *Cdk2ap1*$^{-/-}$ mESC levels. However, in *Cdk2ap1*$^{-/-}$ mESCs, the Wnt signaling could not be further activated with LiCl treatment indicating that Wnt signaling in the knock-out cells was at its biological maximum (Fig. 4*d*).

To understand the mechanism for the increased Y489 shown in *Cdk2ap1*$^{-/-}$ mESCs, we examined adenomatous polyposis coli (APC). The main function of APC includes promoting degradation of β-catenin and chaperoning β-catenin in nuclear-cytoplasmic shuttling. We observed an increase in APC protein level in *Cdk2ap1*$^{-/-}$ compared with WT (Fig. 4*e*). Overexpression of APC could lead to more available APC to shuttle β-catenin to the nucleus, which in turn may explain accumulation of Y489 seen in *Cdk2ap1*$^{-/-}$ mESCs.

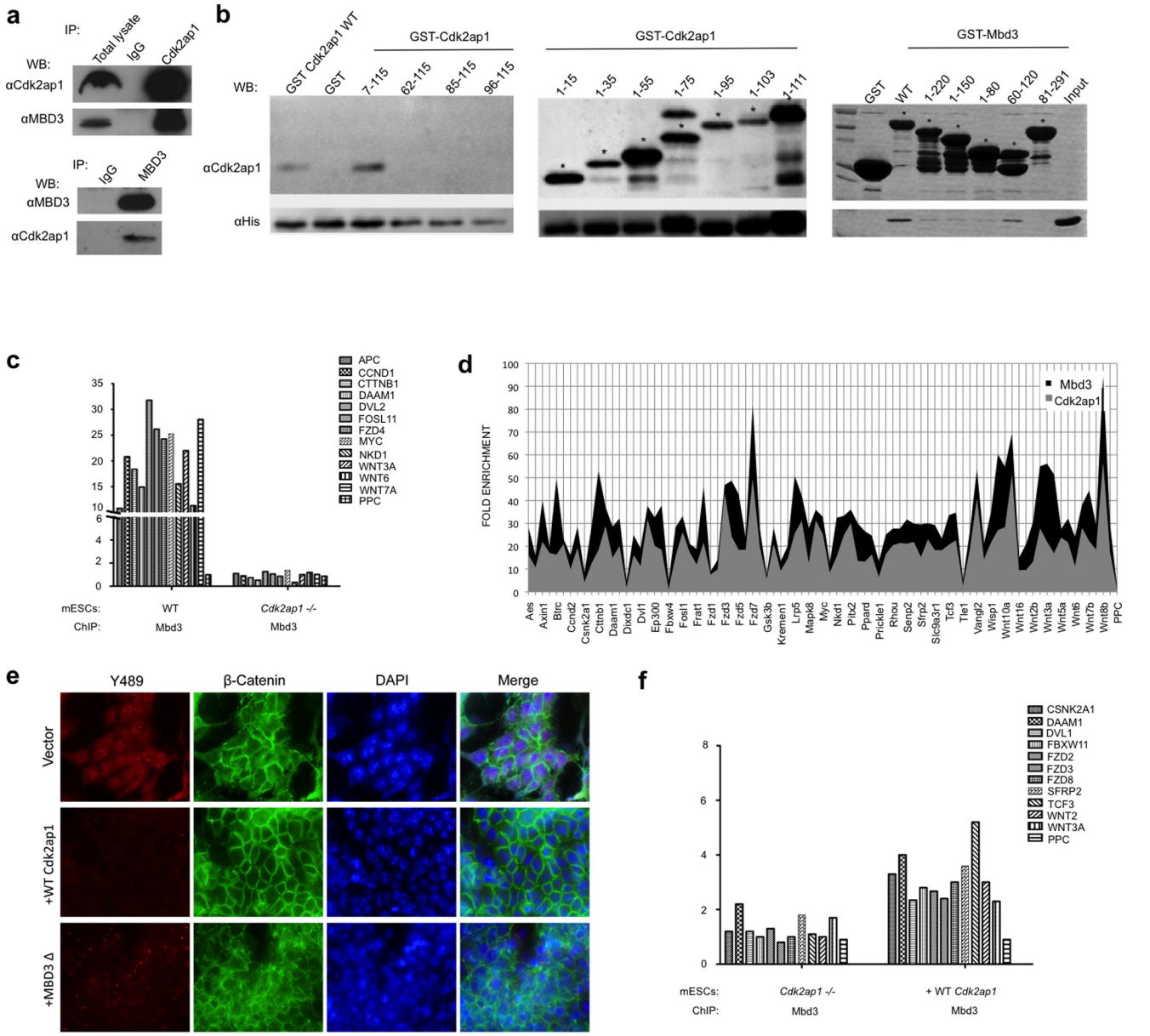

FIGURE 5. **CDK2AP1 is a crucial part of NuRD complex and deletion of *Cdk2ap1* leads to decrease in MBD3-NuRD complex binding abilities to promoters of Wnt genes.** *a*, co-immunoprecipitation between CDK2AP1 and MBD3. *Upper panels*, IP with αCDK2AP1 shows a specific pulldown of MBD3. *Lower panels*, IP with αMBD3 shows a pulldown of CDK2AP1. *b*, creation and co-IP of CDK2AP1-MBD3 binding mutants. *Left* and *middle panels*, using GST-tagged WT *Cdk2ap1* and binding mutants, *in vitro* binding assay shows binding in WT, 7–115, 1–15, 1–35, 1–55, 1–75, 1–95, 1–103, and 1–111. 62–115, 85–115, and 96–115 mutants lose the interaction. *Right panel*, using GST-tagged WT *Mbd3* and binding mutants, the assay shows lost of binding in 81–291 mutant only. *c*, ChIP analysis for MBD3 on eight Wnt gene promoter regions in WT and *Cdk2ap1*$^{-/-}$. *y* axis presents fold enrichment based on MBD3/IgG. Positive PCR Control (PPC) is used as a control. *d*, ChIP analysis for CDK2AP1 and MBD3 on 42 Wnt gene promoter regions in WT mESCs. *y* axis presents fold enrichment based on Mbd3/IgG. Positive PCR Control (PPC) is used as a control. *e*, immunofluorescence microscopy for Y489 (*red*) and total β-catenin (*green*) in lentivirus transduction control (vector), lentivirus-*cdk2ap1* transduced (+WT *Cdk2ap1*) and LV-*Cdk2ap1*-Mbd3 binding mutant transduced (+MBD3Δ) *Cdk2ap1*$^{-/-}$ mESCs. *f*, ChIP analysis for MBD3 on Wnt gene promoter regions in *Cdk2ap1*$^{-/-}$ and *Cdk2ap1* restored *Cdk2ap1*$^{-/-}$ mESCs. *WB*, Western blot.

Taken together, we found that deletion of *Cdk2ap1* leads to hyperactivation of Wnt signaling pathway with increased level of nuclear Y489, up-regulation of c-Myc (downstream effector of Wnt), increased level of the β-catenin chaperoning protein APC, and induction of TCF-LEF luciferase activity. These data clearly demonstrated that the Wnt pathway is deregulated in *Cdk2ap1*$^{-/-}$ mESCs, which may be the cause for their loss of differentiation potentials.

Deletion of CDK2AP1 Leads to a Decrease in the Binding of MBD3 to Promoters of Wnt Genes—It has been shown that CDK2AP1 is a part of the NuRD complex (24, 38, 41). To determine whether CDK2AP1 interacts with MBD3, a major component of the NuRD complex, *in vivo* and *in vitro*, we performed various immunoprecipitation assays of CDK2AP1 and MBD3, finding that the two proteins were able to interact *in vivo* and directly interact *in vitro* (Fig. 5*a*). To find the exact binding domain of CDK2AP1 and MBD3, we generated binding mutants (Fig. 5*b*). By measuring the binding capacity of different GST-tagged CDK2AP1 mutants, we found that MBD3 binds to amino acids 7–15 of CDK2AP1 (Fig. 5*b*, *left* and *middle panels*). By measuring binding capacity of GST-tagged MBD3 mutants (42), we found that CDK2AP1 bound to amino acids

60–81 of MBD3 (Fig. 5*b*, *right panel*). These experiments once again confirmed direct interaction between CDK2AP1 and MBD3 and allowed us to locate specific binding domains.

Our immediate question was then how deletion of Cdk2ap1 resulted in significant DNA methylation changes as demonstrated by DNA methylation analysis. Because CDK2AP1 itself has no DNA methylation activity, we speculate that these DNA methylation changes are due in part to its interacting partner MBD3, which has been shown to affect DNA methylation by Hendrich's and Fazzio's groups (39, 43). Based on our findings, we hypothesize that MBD3 may occupy the promoters of the same genes that are affected by CDK2AP1. To address this, we performed chromatin immunoprecipitation (ChIP) assay for MBD3 on 84 Wnt gene promoters either with or without *Cdk2ap1* (Fig. 5*c*). We found that deletion of *Cdk2ap1* led to a significant decrease in the binding of MBD3 to Wnt gene promoters. This data suggests that certain set of Wnt genes are epigenetically affected by both CDK2AP1 and MBD3. When we examined the binding profiles, it was found that MBD3 and CDK2AP1 shared a very similar binding tendency on the Wnt gene promoters (Fig. 5*d*). Moreover, we found that the interaction between CDK2AP1 and MBD3 was functionally relevant to the deregulation of Wnt in *Cdk2ap1*$^{-/-}$ mESCs. We introduced either WT or MBD3 binding mutant (*Mbd3*Δ) form of *Cdk2ap1* to *Cdk2ap1*$^{-/-}$ mESCs (Fig. 5*e*). We observed an ectopic expression of WT *Cdk2ap1* resulted in a significant decrease of Y489 to the level in WT *Cdk2ap1* mESCs. But the *Mbd3*Δ did not fully restore Y489 to the level in WT *Cdk2ap1* mESCs (Fig. 5*e*). This demonstrates that the recruitment of MBD3 to the promoter region of several important Wnt pathway genes requires CDK2AP1 and the interaction between CDK2AP1-MBD3 is functionally important in the regulation of Wnt in mESCs. Furthermore, when we reintroduced *Cdk2ap1* into the *Cdk2ap1*$^{-/-}$ mESCs, the occupancy of MBD3 to the promoters was restored to a certain level (Fig. 5*f*). The limited level of restoration we observed suggests that the binding of MBD3 may require other factors than CDK2AP1. Also, it is possible that deletion of *Cdk2ap1* may have directed cells to the stage where the full restoration of the binding could not be established. Collectively, the molecular interaction and the promoter occupancy support that the association of MBD3 and CDK2AP1 on Wnt gene promoters is functionally significant in the epigenetic regulation of Wnt signaling in mESCs.

Knockdown of Apc in Cdk2ap1$^{-/-}$ *mESCs Restores WT Phenotype*—To validate the microarray and to find the top candidates for *Cdk2ap1*-mediated Wnt activation, we performed Wnt-focused expression arrays (Fig. 6). We found 12 genes that are significantly overexpressed in *Cdk2ap1*$^{-/-}$ mESCs (Fig. 6, *a* and *b*). We ranked the top eight genes in *Cdk2ap1*$^{-/-}$ mESCs that showed reversible changes to the WT mESC levels upon reintroduction of the wild type *Cdk2ap1* but not the mutant *Cdk2ap1* (*Mbd3*Δ). Therefore, the regulation of these eight genes should be specific to the CDK2AP1-MBD3 interaction (Fig. 6*c*). Based on our differential gene expression and restoration data, we identified *Wnt3a*, *Apc*, and c-*myc* as top candidate Wnt genes that were epigenetically deregulated and functionally important in hyperactivation of Wnt signaling in *Cdk2ap1*$^{-/-}$ mESCs.

To assess the functional significance of one of our candidate Wnt genes in *Cdk2ap1*$^{-/-}$ mESCs, we performed knockdown experiments using siRNA specific to *Apc* and measured the changes in morphology and OCT4 expression levels. We found that knocking down *Apc* restored the differentiation potential in *Cdk2ap1*$^{-/-}$ mESCs to WT levels (Fig. 7). After removal of Leukemia Inhibitory Factor (LIF) for 48 h, the control *Cdk2ap1*$^{-/-}$ mESCs remained pluripotent as expected, which can be evidenced by both morphology and high levels of OCT4 (Fig. 7, *a* and *b*). However, after knocking down *Apc* in the *Cdk2ap1*$^{-/-}$ mESCs, we observed a majority of the cells differentiating into embryoid bodies, a decrease in OCT4 expression, and a decrease in Y489 levels similar to WT cells (Fig. 7, *a*–*d*). This demonstrated that the epigenetic deregulation of *Apc* in *Cdk2ap1*$^{-/-}$ mESCs was functionally relevant to the activation of Wnt in *Cdk2ap1*$^{-/-}$ mESCs. The deregulated Wnt signaling activity in *Cdk2ap1*$^{-/-}$ mESCs may cause cells to be Leukemia Inhibitory Factor (LIF)-independent and remain as self-renewing undifferentiated even under differentiation conditions.

NuRD, Differentiation, and Wnt in Relation to Cdk2ap1 in a Global Context—Bioinformatically, we have examined whether the NuRD complex, ESC differentiation, and Wnt signaling pathway are molecularly interconnected with each other and also with CDK2AP1. We have analyzed gene expression array database on publically available datasets (39, 44–50) representing nucleosome remodeling, stem cell differentiation, and Wnt signaling and compared them to our *Cdk2ap1* gene expression data (Fig. 8). We have constructed a complete metanetwork map of mESCs built from 12 different mouse gene expression arrays to explain how nucleosome remodeling, differentiation, and Wnt signaling pathways are interconnected and linked to CDK2AP1. This global analysis can be used as a platform to further understand the roles of these various pathways within the context of stemness, Wnt, and epigenetics.

DISCUSSION

Understanding the regulatory circuitry of pluripotency has been the main focus in the field of stem cell biology. Advances in the generation of the induced pluripotent stem cells show that the pluripotent state is largely controlled by few core transcription factors, OCT4, KLF4, NANOG, and SOX2 (51). However, the practical use of stem cells for regenerative medicine still hinges upon the understanding of the mechanism underlying the differentiation process. Recently, our understanding of the dynamic role of NuRD in the regulation of stem cells has begun to explain the fundamental mechanisms of pluripotency (35, 39, 52, 53). Reynolds *et al.* (52) showed that NuRD is required for ESC lineage commitment and modulates transcriptional heterogeneity for pluripotency genes. However, stem cell regulation by NuRD still remains largely elusive (35). The mode of interaction between NuRD and gene promoters is a fundamental yet important unanswered question. In this study, we found a novel regulatory factor within the NuRD complex, which may function as a guide in NuRD recruitment to specific Wnt genes to regulate stem cell pluripotency.

Using DNA methylation and gene expression profiling, we identified Wnt as a key pluripotency pathway that may play a critical role in NuRD-regulated ESC self-renewal. Using

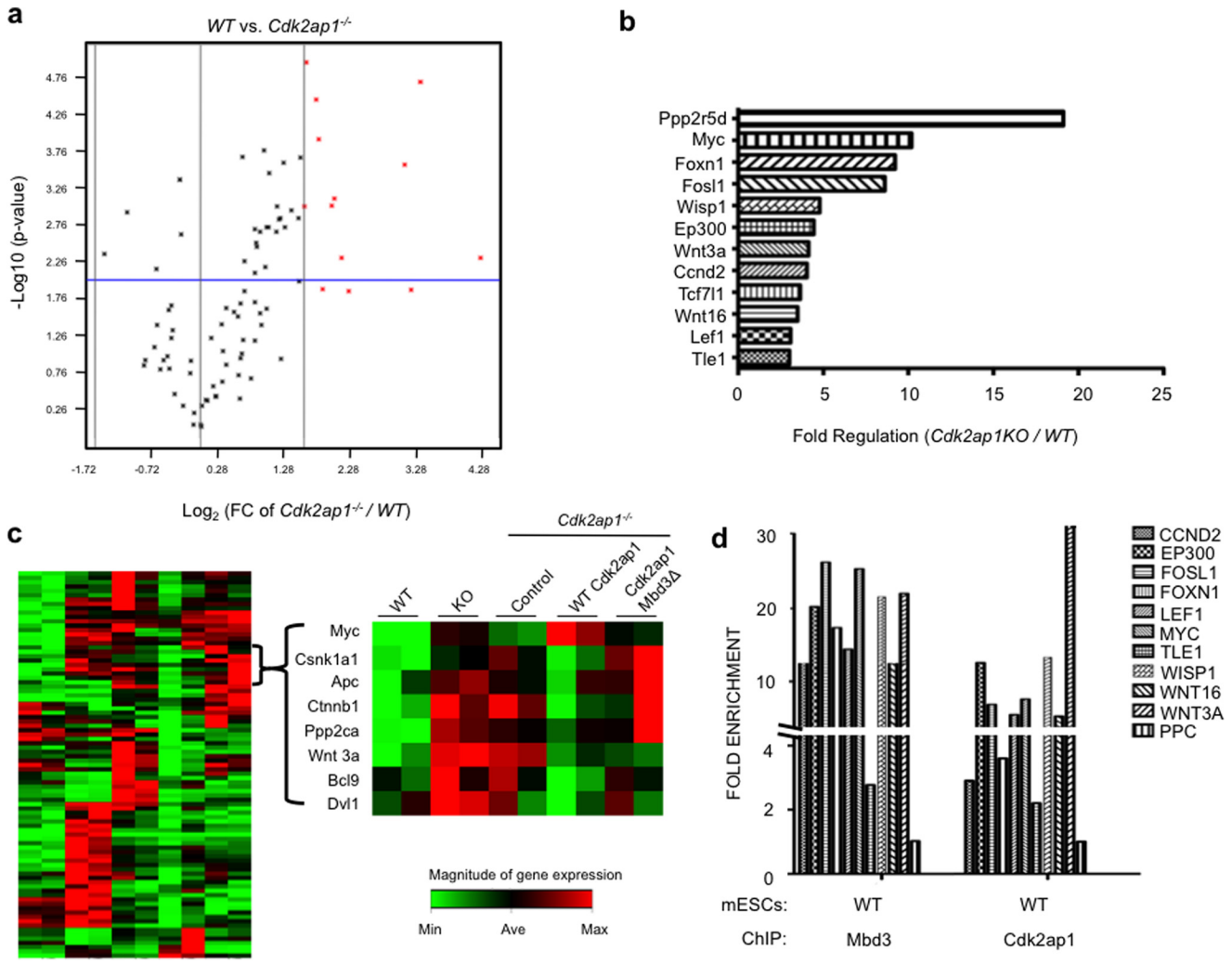

FIGURE 6. **Wnt expression array confirms loss of occupancy in *Cdk2ap1*$^{-/-}$ mESCs and identifies *Wnt3a*, *Apc*, and c-*myc* as top targets of *Cdk2ap1*-mediated Wnt activation.** *a*, Wnt-focused expression arrays utilizing WT and *Cdk2ap1*$^{-/-}$ mESCs. The *x* axis represents fold change of *Cdk2ap1*$^{-/-}$/WT and *y* axis represents *p* value. 12 statically significant genes are shown in *red*. *b*, 12 genes that are overexpressed in *Cdk2ap1*$^{-/-}$ mESCs based on significant *p* value and fold change are listed here. *x* axis represents gene names and *y* axis represents fold regulation based on *Cdk2ap1*$^{-/-}$ over WT. *c*, Heat map showing clustering analysis of WT, *Cdk2ap1*$^{-/-}$, restoration control, WT *Cdk2ap1* restoration, and *Cdk2ap1*(*Mbd3*Δ) restoration. Of the 84 Wnt genes, the top eight genes that could be restored back to WT levels by ectopic expression of wild type *Cdk2ap1*, but not by control or mutant *Cdk2ap1* (*Mbd3*Δ) in *Cdk2ap1*$^{-/-}$ mESCs are expanded to the right of the heatmap. *d*, ChIP analysis for CDK2AP1 and MBD3 on 10 Wnt gene promoter regions that are statically differentially expressed between WT and *Cdk2ap1*$^{-/-}$ mESCs. *y* axis presents fold enrichment based on MBD3/IgG. PPC is used as a control. *Min*, minimum; *Ave*, average; *Max*, maximum.

Cdk2ap1$^{-/-}$ mESCs, we found that disruption in the interaction between CDK2AP1 and MBD3 led to epigenetic changes in a significant number of Wnt pathway genes. Our data have demonstrated that Wnt signaling is under precise control through CDK2AP1-MBD3 in mESCs. When the nucleosome remodeling complex was disrupted by deletion of *Cdk2ap1*, the epigenetic control of Wnt signaling was lost. The epigenetic changes resulted in corresponding mRNA level changes in Wnt genes, including *Apc*, *Wnt3a*, and c-*myc* and also changes in protein level of Wnt signaling molecules such as active nuclear p-β-catenin (Y489). Increased Y489 led to an increase in TCF-LEF transcriptional activity, which resulted in hyperactivation of Wnt. The hyperactivity may promote expression of pluripotency specific genes, which is the phenotype seen in *Cdk2ap1*$^{-/-}$ mESCs.

Because it is clear that the delicate balance of Wnt signaling is necessary for normal regulation of stem cells, we hypothesized that there had to be a Wnt target that could be modulated to restore a normal phenotype in *Cdk2ap1*$^{-/-}$ mESCs. To find the targets that were not only CDK2AP1-mediated but also through CDK2AP1-MBD3 interaction, we compared significant gene expression changes between WT and *Cdk2ap1*$^{-/-}$ mESCs. Moreover, we identified Wnt gene targets whose gene expression could be restored back to WT mESCs by ectopic expression of wild type *Cdk2ap1*, but not by mutant *Cdk2ap1* (*Mbd3*Δ) in *Cdk2ap1*$^{-/-}$ mESCs. In *Cdk2ap1*$^{-/-}$ mESCs, there was a significant up-regulation of APC compared with WT mESCs, which made APC an ideal target. Knocking down *Apc* led to the restoration in differentiation potential in *Cdk2ap1*$^{-/-}$ mESCs by embryoid body formation and decrease in OCT4 expression. This is very interesting because a previous study had shown that lack of *Apc* leads to loss of differentiation in mESCs (54). Here, we show for the first time that an up-regulation of *Apc* could lead to sustained pluripotency in mESCs

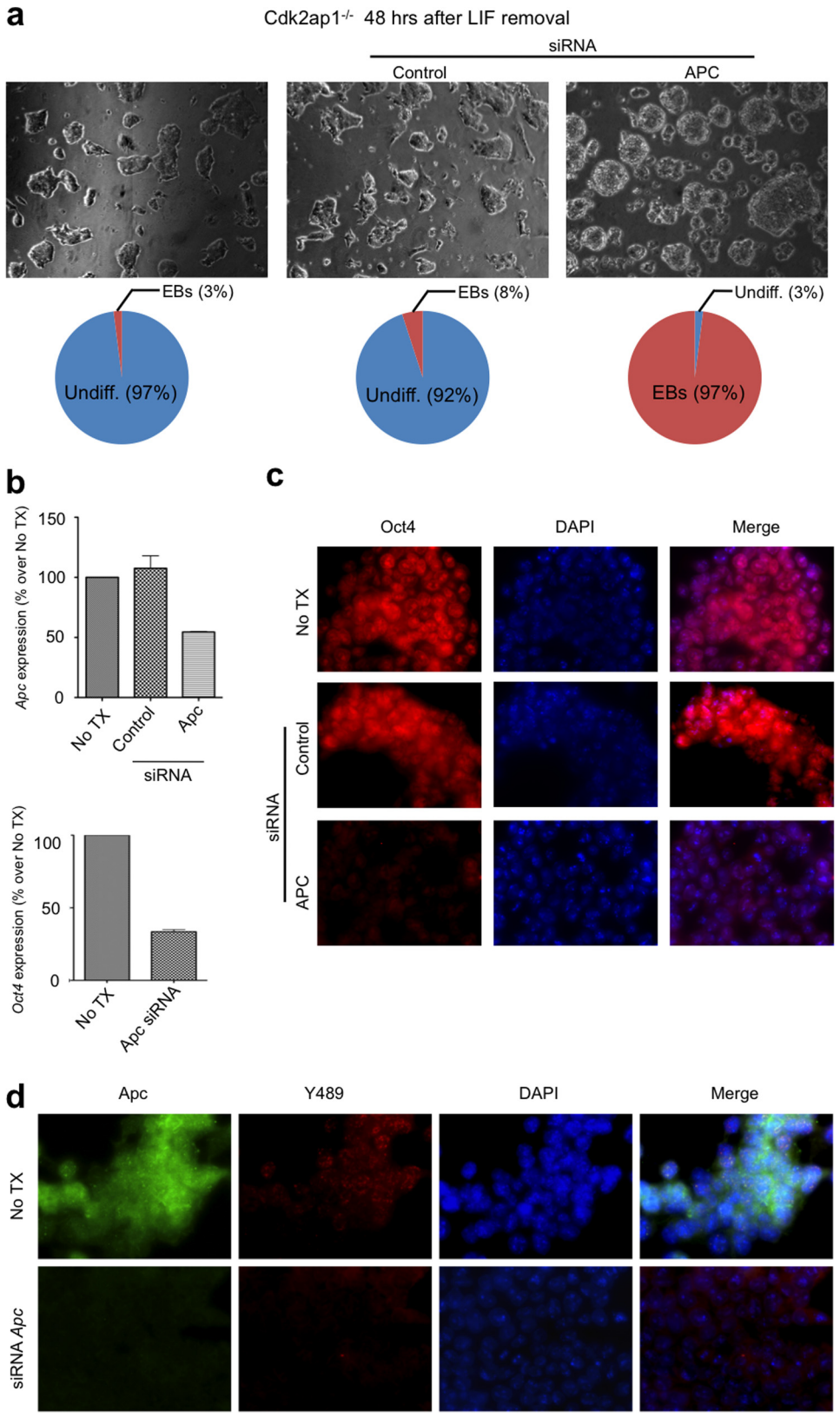

FIGURE 7. **Knockdown of *Apc* by siRNA in *Cdk2ap1*$^{-/-}$ mESCs restores differential competency.** *a*, siRNA experiment by knocking down *Apc* in *Cdk2ap1*$^{-/-}$ mESCs. *Left panel*, *Cdk2ap1*$^{-/-}$ mESCs stay undifferentiated (*Undiff.*) even after LIF removal (97% undifferentiated stem cells). *Middle panel*, *Cdk2ap1*$^{-/-}$ mESCs stay undifferentiated even after LIF removal with control siRNA (92% undifferentiated stem cells). *Right panel*, *Cdk2ap1*$^{-/-}$ mESCs differentiate into embryoid bodies (*EBs*) after LIF removal with *Apc* siRNA (97% embryoid bodies). *b*, immunofluorescence microscopy for Oct4 (*red*) in *Cdk2ap1*$^{-/-}$ mESCs with and without *Apc* siRNA. *TX*, Transfection. *c*, quantitative PCR showing decreased expression of *Oct4* in *Apc* siRNA knockdown compared with WT and control siRNA. *d*, immunofluorescence microscopy for Apc (*green*) and Y489 (*red*) in *Cdk2ap1*$^{-/-}$ mESCs with and without *Apc* siRNA. Apc protein expression and Y489 protein expression decrease with *Apc* siRNA in *Cdk2ap1*$^{-/-}$ mESCs. *e*, qPCR showing decreased expression of *Apc* in *Apc* siRNA knockdown compared with WT and control siRNA.

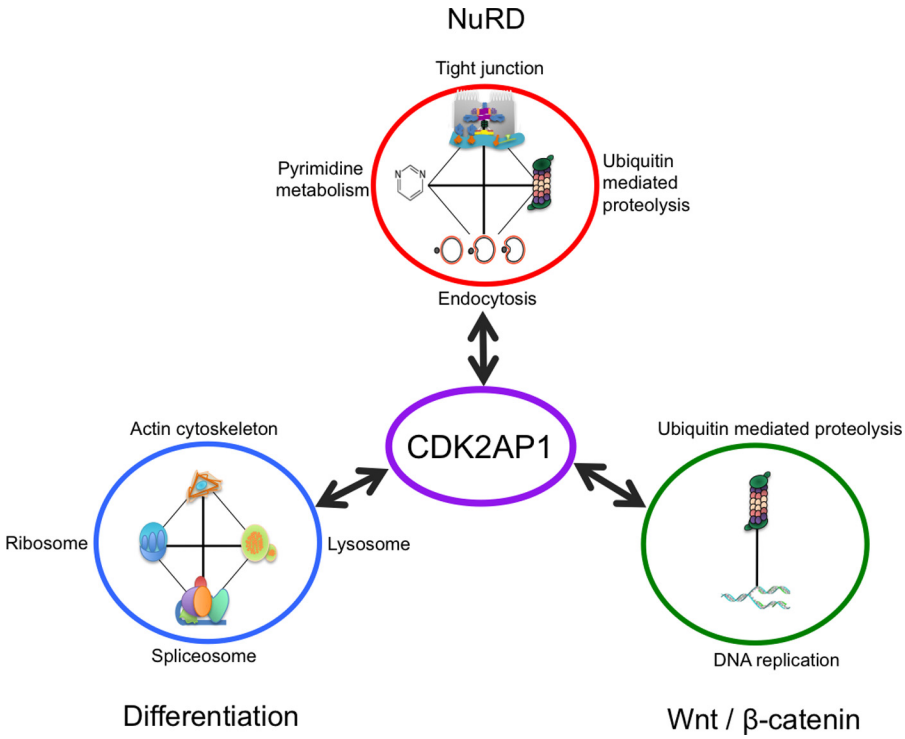

FIGURE 8. **NuRD, differentiation, and Wnt in relation to Cdk2ap1 in a global context.** A complete metanetwork map of mESCs to explain how nucleosome remodeling, differentiation, and Wnt signaling pathway are interconnected and linked to CDK2AP1.

and knocking down *Apc* resulted in down-regulation of Y489, which may suggest the role of APC as β-catenin chaperone to be more complicated than described previously (55). Up-regulation of *Apc* in the cytoplasm and up-regulation of Y489 seen in *Cdk2ap1*$^{-/-}$ mESCs suggest that there might be an unknown regulatory element that cues translocation of APC into the nucleus to chaperone β-catenin for cytoplasmic degradation other than B56α or defective nuclear localization signals on the ARM domain of APC (56).

Taken together, we show that alteration of NuRD by deletion of *Cdk2ap1* leads to activation of Wnt signaling, which in turn decreases stem cell differentiation potential. The manner in which CDK2AP1 affects the recruitment of MBD3 is site-specific and not randomly occurring throughout the genome. We believe that this site-specific role of MBD3 has to do with a complex interplay of associated proteins, in our case, CDK2AP1. Our data suggests that NuRD may be similar to RNA polymerase II, which is responsible for tens of thousands of transcripts mediated by a network of sequence-specific DNA binding proteins (57). These binding factors can guide RNA polymerase II in a site-specific manner (57). Similarly, our findings imply that NuRD is not randomly distributed on methylated cytosines but instead may be more site-specific than described previously. It would be imperative to find out what other sequence-specific factors exist; the locations and patterns in the genome they may occupy; and in a broader sense, how regulation of the nucleosome remodeling complex relates to transcription control.

Previously, others have shown the role of Wnt and p-β-catenin in stem cell pluripotency and differentiation potential. In fact, there have been controversies surrounding the exact role that Wnt may play in ESCs (58). Here, we have demonstrated that maintenance of mESC pluripotency is under epigenetic control of the Wnt pathway. Moreover, we observed the site-specific role of MBD3 with a complex interplay of CDK2AP1 on the promoters of Wnt singling genes. We also presented for the first time unique gene signatures responsible in Wnt signaling, differentiation, and nucleosome remodeling useful in defining the biological pathways involved in stem cell identity. We believe elucidating this link between NuRD, Wnt, and differentiation may enable us to ultimately control self-renewal in embryonic stem cells. Furthermore, understanding Wnt controlled stem cell pluripotency and the role of CDK2AP1-MBD3-NuRD complex at the molecular level may largely contribute to current knowledge of basic stem cell biology as well as future application to regenerative therapies.

Acknowledgments—We thank Dr. Steve Horvath (UCLA) for helping with the WGCNA analysis and Dr. Gary Hon (University of California, San Diego) for data matrix scripts. We are also thankful to Dr. Timothy Lane (UCLA) for helpful Wnt-related suggestions. We acknowledge the Clinical Microarray and the Vector Core at UCLA for excellent technical service.

REFERENCES

1. Schroeder, I. S. (2012) Potential of pluripotent stem cells for diabetes therapy. *Curr. Diabetes Rep.* **5,** 490–498
2. Lindvall, O., Kokaia, Z., and Martinez-Serrano, A. (2004) Stem cell therapy for human neurodegenerative disorders-how to make it work. *Nat. Med.* **10,** S42–50
3. Kim, S. U., and de Vellis, J. (2009) Stem cell-based cell therapy in neurological diseases: a review. *J. Neurosci. Res.* **87,** 2183–2200
4. Segers, V. F., and Lee, R. T. (2008) Stem-cell therapy for cardiac disease. *Nature* **451,** 937–942
5. Keirstead, H. S., Nistor, G., Bernal, G., Totoiu, M., Cloutier, F., Sharp, K.,

and Steward, O. (2005) Human embryonic stem cell-derived oligodendrocyte progenitor cell transplants remyelinate and restore locomotion after spinal cord injury. *J. Neurosci.* **25,** 4694–4705
6. Hu, Q., Friedrich, A. M., Johnson, L. V., and Clegg, D. O. (2010) Memory in induced pluripotent stem cells: reprogrammed human retinal-pigmented epithelial cells show tendency for spontaneous redifferentiation. *Stem Cells* **28,** 1981–1991
7. Discher, D. E., Mooney, D. J., and Zandstra, P. W. (2009) Growth factors, matrices, and forces combine and control stem cells. *Science* **324,** 1673–1677
8. Fuchs, E., Tumbar, T., and Guasch, G. (2004) Socializing with the neighbors: stem cells and their niche. *Cell* **116,** 769–778
9. Bibikova, M., Laurent, L. C., Ren, B., Loring, J. F., and Fan, J. B. (2008) Unraveling epigenetic regulation in embryonic stem cells. *Cell Stem Cell* **2,** 123–134
10. Bernstein, B. E., Mikkelsen, T. S., Xie, X., Kamal, M., Huebert, D. J., Cuff, J., Fry, B., Meissner, A., Wernig, M., Plath, K., Jaenisch, R., Wagschal, A., Feil, R., Schreiber, S. L., and Lander, E. S. (2006) A bivalent chromatin structure marks key developmental genes in embryonic stem cells. *Cell* **125,** 315–326
11. Hattori, N., Nishino, K., Ko, Y. G., Hattori, N., Ohgane, J., Tanaka, S., and Shiota, K. (2004) Epigenetic control of mouse Oct-4 gene expression in embryonic stem cells and trophoblast stem cells. *J. Biol. Chem.* **279,** 17063–17069
12. Meshorer, E., and Misteli, T. (2006) Chromatin in pluripotent embryonic stem cells and differentiation. *Nat. Rev. Mol. Cell Biol.* **7,** 540–546
13. Bibikova, M., Chudin, E., Wu, B., Zhou, L., Garcia, E. W., Liu, Y., Shin, S., Plaia, T. W., Auerbach, J. M., Arking, D. E., Gonzalez, R., Crook, J., Davidson, B., Schulz, T. C., Robins, A., Khanna, A., Sartipy, P., Hyllner, J., Vanguri, P., Savant-Bhonsale, S., Smith, A. K., Chakravarti, A., Maitra, A., Rao, M., Barker, D. L., Loring, J. F., and Fan, J. B. (2006) Human embryonic stem cells have a unique epigenetic signature. *Genome Res.* **16,** 1075–1083
14. Chung, Y. S., Kim, H. J., Kim, T. M., Hong, S. H., Kwon, K. R., An, S., Park, J. H., Lee, S., and Oh, I. H. (2009) Undifferentiated hematopoietic cells are characterized by a genome-wide undermethylation dip around the transcription start site and a hierarchical epigenetic plasticity. *Blood* **114,** 4968–4978
15. Hashimshony, T., Zhang, J., Keshet, I., Bustin, M., and Cedar, H. (2003) The role of DNA methylation in setting up chromatin structure during development. *Nat. Genet.* **34,** 187–192
16. Lorincz, M. C., Dickerson, D. R., Schmitt, M., and Groudine, M. (2004) Intragenic DNA methylation alters chromatin structure and elongation efficiency in mammalian cells. *Nat. Struct. Mol. Biol.* **11,** 1068–1075
17. Zhang, Y., Ng, H. H., Erdjument-Bromage, H., Tempst, P., Bird, A., and Reinberg, D. (1999) Analysis of the NuRD subunits reveals a histone deacetylase core complex and a connection with DNA methylation. *Genes Dev.* **13,** 1924–1935
18. Kaji, K., Nichols, J., and Hendrich, B. (2007) Mbd3, a component of the NuRD co-repressor complex, is required for development of pluripotent cells. *Development* **134,** 1123–1132
19. Shintani, S., Ohyama, H., Zhang, X., McBride, J., Matsuo, K., Tsuji, T., Hu, M. G., Hu, G., Kohno, Y., Lerman, M., Todd, R., and Wong, D. T. (2000) p12(DOC-1) is a novel cyclin-dependent kinase 2-associated protein. *Mol. Cell Biol.* **20,** 6300–6307
20. Todd, R., McBride, J., Tsuji, T., Donoff, R. B., Nagai, M., Chou, M. Y., Chiang, T., and Wong, D. T. (1995) Deleted in oral cancer-1 (doc-1), a novel oral tumor suppressor gene. *FASEB J.* **9,** 1362–1370
21. Kim, Y., McBride, J., Kimlin, L., Pae, E. K., Deshpande, A., and Wong, D. T. (2009) Targeted inactivation of p12, CDK2 associating protein 1, leads to early embryonic lethality. *PLoS One* **4,** e4518
22. Deshpande, A. M., Dai, Y. S., Kim, Y., Kim, J., Kimlin, L., Gao, K., and Wong, D. T. (2009) Cdk2ap1 is required for epigenetic silencing of Oct4 during murine embryonic stem cell differentiation. *J. Biol. Chem.* **284,** 6043–6047
23. Kim, Y., Deshpande, A., Dai, Y., Kim, J. J., Lindgren, A., Conway, A., Clark, A. T., and Wong, D. T. (2009) Cyclin-dependent kinase 2-associating protein 1 commits murine embryonic stem cell differentiation through retinoblastoma protein regulation. *J. Biol. Chem.* **284,** 23405–23414
24. Le Guezennec, X., Vermeulen, M., Brinkman, A. B., Hoeijmakers, W. A., Cohen, A., Lasonder, E., and Stunnenberg, H. G. (2006) MBD2/NuRD and MBD3/NuRD, two distinct complexes with different biochemical and functional properties. *Mol. Cell Biol.* **26,** 843–851
25. Gat, U., DasGupta, R., Degenstein, L., and Fuchs, E. (1998) De Novo hair follicle morphogenesis and hair tumors in mice expressing a truncated beta-catenin in skin. *Cell* **95,** 605–614
26. Huelsken, J., Vogel, R., Erdmann, B., Cotsarelis, G., and Birchmeier, W. (2001) beta-Catenin controls hair follicle morphogenesis and stem cell differentiation in the skin. *Cell* **105,** 533–545
27. Chenn, A., and Walsh, C. A. (2002) Regulation of cerebral cortical size by control of cell cycle exit in neural precursors. *Science* **297,** 365–369
28. Zechner, D., Fujita, Y., Hülsken, J., Müller, T., Walther, I., Taketo, M. M., Crenshaw, E. B., 3rd, Birchmeier, W., and Birchmeier, C. (2003) β-Catenin signals regulate cell growth and the balance between progenitor cell expansion and differentiation in the nervous system. *Dev. Biol.* **258,** 406–418
29. Sato, N., Meijer, L., Skaltsounis, L., Greengard, P., and Brivanlou, A. H. (2004) Maintenance of pluripotency in human and mouse embryonic stem cells through activation of Wnt signaling by a pharmacological GSK-3-specific inhibitor. *Nat. Med.* **10,** 55–63
30. Sambrook, J., and Russell, D. W. (2006) Rapid isolation of yeast DNA. *CSH Protoc.* **1**
31. Mohn, F., Weber, M., Schübeler, D., and Roloff, T. C. (2009) Methylated DNA immunoprecipitation (MeDIP). *Methods Mol. Biol.* **507,** 55–64
32. Dennis, G., Jr., Sherman, B. T., Hosack, D. A., Yang, J., Gao, W., Lane, H. C., and Lempicki, R. A. (2003) DAVID: database for annotation, visualization, and integrated discovery. *Genome. Biol.* **4,** P3
33. Maniatis, T., Fritsch, E. F., and Sambrook, J. (1982) *Molecular cloning: a laboratory manual*, pp. A8.40–A8.51, Cold Spring Harbor Laboratory, Cold Spring Harbor, NY
34. Langfelder, P., and Horvath, S. (2008) WGCNA: an R package for weighted correlation network analysis. *BMC Bioinformatics* **9,** 559
35. Hu, G., and Wade, P. A. (2012) NuRD and pluripotency: a complex balancing act. *Cell Stem Cell* **10,** 497–503
36. Maunakea, A. K., Nagarajan, R. P., Bilenky, M., Ballinger, T. J., D'Souza, C., Fouse, S. D., Johnson, B. E., Hong, C., Nielsen, C., Zhao, Y., Turecki, G., Delaney, A., Varhol, R., Thiessen, N., Shchors, K., Heine, V. M., Rowitch, D. H., Xing, X., Fiore, C., Schillebeeckx, M., Jones, S. J., Haussler, D., Marra, M. A., Hirst, M., Wang, T., and Costello, J. F. (2010) Conserved role of intragenic DNA methylation in regulating alternative promoters. *Nature* **466,** 253–257
37. Tate, P. H., and Bird, A. P. (1993) Effects of DNA methylation on DNA-binding proteins and gene expression. *Curr. Opin. Genet. Dev.* **3,** 226–231
38. Spruijt, C. G., Bartels, S. J., Brinkman, A. B., Tjeertes, J. V., Poser, I., Stunnenberg, H. G., and Vermeulen, M. (2010) *Mol. Biosyst.* **6,** 1700–1706
39. Yildirim, O., Li, R., Hung, J. H., Chen, P. B., Dong, X., Ee, L. S., Weng, Z., Rando, O. J., and Fazzio, T. G. (2011) Mbd3/NURD complex regulates expression of 5-hydroxymethylcytosine marked genes in embryonic stem cells. *Cell* **147,** 1498–1510
40. Rhee, J., Buchan, T., Zukerberg, L., Lilien, J., and Balsamo, J. (2007) Cables links Robo-bound Abl kinase to *N*-cadherin-bound β-catenin to mediate Slit-induced modulation of adhesion and transcription. *Nat. Cell Biol.* **9,** 883–892
41. Reddy, B. A., Bajpe, P. K., Bassett, A., Moshkin, Y. M., Kozhevnikova, E., Bezstarosti, K., Demmers, J. A., Travers, A. A., and Verrijzer, C. P. (2010) Drosophila transcription factor Tramtrack69 binds MEP1 to recruit the chromatin remodeler NuRD. *Mol. Cell Biol.* **30,** 5234–5244
42. Jin, S. G., Jiang, C. L., Rauch, T., Li, H., and Pfeifer, G. P. (2005) MBD3L2 interacts with MBD3 and components of the NuRD complex and can oppose MBD2-MeCP1-mediated methylation silencing. *J. Biol. Chem.* **280,** 12700–12709
43. Latos, C. H., Olukunbi, M, Dominika, A. D, Bryony, Stubbs, M B, Manel, E and Brian, H. (2012) NuRD-dependent DNA methylation prevents ES cells from accessing a trophectoderm fate. *Biology Open* 1, 341–352
44. Bridgewater, D., Cox, B., Cain, J., Lau, A., Athaide, V., Gill, P. S., Kuure, S., Sainio, K., and Rosenblum, N. D. (2008) Canonical WNT/β-catenin signaling is required for ureteric branching. *Dev. Biol.* **317,** 83–94

45. Fevr, T., Robine, S., Louvard, D., and Huelsken, J. (2007) Wnt/β-catenin is essential for intestinal homeostasis and maintenance of intestinal stem cells. *Mol. Cell Biol.* **27,** 7551–7559
46. Collins, C. A., Kretzschmar, K., and Watt, F. M. (2011) Reprogramming adult dermis to a neonatal state through epidermal activation of β-catenin. *Development* **138,** 5189–5199
47. Ema, M., Mori, D., Niwa, H., Hasegawa, Y., Yamanaka, Y., Hitoshi, S., Mimura, J., Kawabe, Y., Hosoya, T., Morita, M., Shimosato, D., Uchida, K., Suzuki, N., Yanagisawa, J., Sogawa, K., Rossant, J., Yamamoto, M., Takahashi, S., and Fujii-Kuriyama, Y. (2008) Krüppel-like factor 5 is essential for blastocyst development and the normal self-renewal of mouse ESCs. *Cell Stem Cell* **3,** 555–567
48. Sinkkonen, L., Hugenschmidt, T., Berninger, P., Gaidatzis, D., Mohn, F., Artus-Revel, C. G., Zavolan, M., Svoboda, P., and Filipowicz, W. (2008) MicroRNAs control *de novo* DNA methylation through regulation of transcriptional repressors in mouse embryonic stem cells. *Nat. Struct. Mol. Biol.* **15,** 259–267
49. Gao, X., Tate, P., Hu, P., Tjian, R., Skarnes, W. C., and Wang, Z. (2008) ES cell pluripotency and germ-layer formation require the SWI/SNF chromatin remodeling component BAF250a. *Proc. Natl. Acad. Sci. U.S.A.* **105,** 6656–6661
50. Loh, Y. H., Wu, Q., Chew, J. L., Vega, V. B., Zhang, W., Chen, X., Bourque, G., George, J., Leong, B., Liu, J., Wong, K. Y., Sung, K. W., Lee, C. W., Zhao, X. D., Chiu, K. P., Lipovich, L., Kuznetsov, V. A., Robson, P., Stanton, L. W., Wei, C. L., Ruan, Y., Lim, B., and Ng, H. H. (2006) The Oct4 and Nanog transcription network regulates pluripotency in mouse embryonic stem cells. *Nat. Genet.* **38,** 431–440
51. Takahashi, K., and Yamanaka, S. (2006) Induction of pluripotent stem cells from mouse embryonic and adult fibroblast cultures by defined factors. *Cell* **126,** 663–676
52. Reynolds, N., Latos, P., Hynes-Allen, A., Loos, R., Leaford, D., O'Shaughnessy, A., Mosaku, O., Signolet, J., Brennecke, P., Kalkan, T., Costello, I., Humphreys, P., Mansfield, W., Nakagawa, K., Strouboulis, J., Behrens, A., Bertone, P., and Hendrich, B. (2012) NuRD suppresses pluripotency gene expression to promote transcriptional heterogeneity and lineage commitment. *Cell Stem Cell* **10,** 583–594
53. Whyte, W. A., Bilodeau, S., Orlando, D. A., Hoke, H. A., Frampton, G. M., Foster, C. T., Cowley, S. M., and Young, R. A. (2012) Enhancer decommissioning by LSD1 during embryonic stem cell differentiation. *Nature* **482,** 221–225
54. Kielman, M. F., Rindapää, M., Gaspar, C., van Poppel, N., Breukel, C., van Leeuwen, S., Taketo, M. M., Roberts, S., Smits, R., and Fodde, R. (2002) Apc modulates embryonic stem-cell differentiation by controlling the dosage of β-catenin signaling. *Nat. Genet.* **32,** 594–605
55. Henderson, B. R. (2000) Nuclear-cytoplasmic shuttling of APC regulates β-catenin subcellular localization and turnover. *Nat. Cell Biol.* **2,** 653–660
56. Galea, M. A., Eleftheriou, A., and Henderson, B. R. (2001) ARM domain-dependent nuclear import of adenomatous polyposis coli protein is stimulated by the B56 α subunit of protein phosphatase 2A. *J. Biol. Chem.* **276,** 45833–45839
57. Kadonaga, J. T. (2004) Regulation of RNA polymerase II transcription by sequence-specific DNA binding factors. *Cell* **116,** 247–257
58. Miki, T., Yasuda, S. Y., and Kahn, M. (2011) Wnt/β-catenin signaling in embryonic stem cell self-renewal and somatic cell reprogramming. *Stem Cell Rev.* **7,** 836–846